

A CATALOG OF CALIBRATOR STARS FOR NEXT-GENERATION OPTICAL INTERFEROMETERS

SAMUEL J. SWIHART¹, E. VICTOR GARCIA^{2,3}, KEIVAN G. STASSUN^{2,4}, GERARD VAN BELLE³, MATTHEW W. MUTTERSPOUGH⁵,
NICHOLAS ELIAS⁶

¹Department of Physics and Astronomy, Michigan State University, East Lansing, MI 48824, USA

²Vanderbilt University, Department of Physics & Astronomy, 6301 Stevenson Center Ln., Nashville, TN 37235, USA

³Lowell Observatory, 1400 W. Mars Hill Rd., Flagstaff, AZ 86001, USA

⁴Fisk University, Department of Physics, 1000 17th Ave. N., Nashville, TN 37208, USA

⁵Tennessee State University, 3500 John A. Merritt Blvd., Nashville, TN 37209, USA

⁶OAM Solutions, LLC, 9300 Stardust Trail, Flagstaff, AZ 86004, USA

The Astronomical Journal, 153:16 (9pp), 2017 January

ABSTRACT

Benchmark stars with known angular diameters are key to calibrating interferometric observations. With the advent of optical interferometry, there is a need for suitably bright, well-vetted calibrator stars over a large portion of the sky. We present a catalog of uniformly computed angular diameters for 1523 stars in the northern hemisphere brighter than $V = 6$ and with declinations $-15^\circ < \delta < 82^\circ$. The median angular stellar diameter is 0.527 mas. The list has been carefully cleansed of all known binary and multiple stellar systems. We derive the angular diameters for each of the stars by fitting spectral templates to the observed spectral energy distributions (SEDs) from literature fluxes. We compare these derived angular diameters against those measured by optical interferometry for 75 of the stars, as well as to 176 diameter estimates from previous calibrator catalogs, finding in general excellent agreement. The final catalog includes our goodness-of-fit metrics as well as an online atlas of our SED fits. The catalog presented here permits selection of the best calibrator stars for current and future visible-light interferometric observations.

1. INTRODUCTION

Optical and infrared interferometry is a powerful tool for directly measuring stellar radii, constraining binary and multiple star orbits, and observing stellar surface features such as rapid rotation or star spots in the milli-arcsecond spatial resolution regime, which is inaccessible by many other observing techniques. In the northern hemisphere there are two operational six-telescope interferometers, the Navy Precision Optical Interferometer (NPOI, [Armstrong et al. 1998](#)) and the Center for High Angular Resolution Astronomy (CHARA, [ten Brummelaar et al. 2005](#)). Each has its own assemblage of different beam combiners, such as the Visible Imaging System for Interferometric Observations (VISION, [Ghasempour et al. 2012](#); [Garcia et al. 2016](#)) and NPOI classic ([Armstrong et al. 1998](#)), at NPOI, and the Michigan Infrared Combiner (MIRC [Monnier et al. 2004](#)), the Precision Astronomical Visible Observations (PAVO, [Ireland et al. 2008](#)), the Visible spEctroGraph and polArimeter (VEGA, [Mourard et al. 2009](#)), and the CLassic Interferometry with Multiple Baselines (CLIMB, [ten Brummelaar et al. 2013](#)) for the CHARA array.

All of these beam combiners measure the basic optical/IR interferometric observables: the squared visibility and/or the closure phase and triple amplitude. To do this, these optical/IR beam combiners require that the instrument's response to a point-source during an observation is well known ([van Belle & van Belle 2005](#)). Typically, these calibrator stars (with known angular diameters) are interleaved with target stars throughout the observation. Without observing a calibrator star with a *known* angular diameter during a sequence of observations of a target star, the squared visibility cannot be calibrated accurately. Additionally, ensuring a calibrator is not in a resolved binary helps guarantee the calibrator closure phases are zero. Thus, using calibrator stars with accurate angular diameters, which are also vetted for known binary systems, lies at the

heart of accurate optical/IR interferometry.

However, often angular diameters for calibrators are obtained in an ad-hoc basis, using a myriad of SED fitting routines or by restricting observations of target stars to ones that have nearby (typically $< 15''$), bright ($V < 6$) calibrator stars with interferometrically measured angular diameters. In this work, we take a *uniform* approach to develop a set of carefully measured angular diameters for 1523 stars brighter than $V = 6$ in the northern hemisphere, vetted for known binary and multiple stellar systems.

In § 2 we provide some brief background for why calibrator stars are vital to doing science using optical interferometry. In § 3 we describe the methods used to pick the ideal sample of calibrators and the process used to construct our final catalog. We utilize spectral energy distribution (SED) fitting to compute the bolometric flux of each star in our list. We require a low reduced χ^2 in order to keep only stars with high quality photometry that covers the entire SED (0.2–10 μm) and which are well-fit by our spectral templates. Results from our SED fits are presented in § 4. In § 5 we compare our derived angular diameters against those measured directly by interferometers and to diameter estimates from previous calibrator catalogs. We provide this list of calibrator stars, together with an online atlas of the SED fits, to the greater interferometry community. Finally, we provide a brief summary of our calibrator sample in § 6.

2. IMPORTANCE OF CALIBRATORS WITH KNOWN ANGULAR DIAMETERS FOR INTERFEROMETRY

As a source increases in apparent size, it becomes more resolved by a fixed interferometric baseline and the squared visibility amplitude decreases. Ideally, the visibility squared of a point source will always be unity. Due to instrumental visibility losses however, the visibility squared measured by a beam combiner for a point source is less than unity. The beam

arXiv:1610.04600v2 [astro-ph.SR] 18 Jun 2017

Table 1
Comparisons of `sedFit` angular diameter estimates for different Pickles spectral template luminosity classes.

HD#	Pickles Spectral Template	$\theta_{\text{SED}} \pm \sigma$ (mas)	χ_{red}^2
HD174464	F2II	0.611 ± 0.051	1.40
	F2III	0.667 ± 0.058	7.30
HD184010	K0III	0.904 ± 0.057	5.93
	K0IV	0.800 ± 0.039	0.65
HD1671	F5IV	0.619 ± 0.030	0.81
	F5V	0.605 ± 0.016	1.10

combiner’s system visibility is:

$$V_{\text{system}}^2(t) = \frac{V_{\text{obs,cal}}^2(t)}{V_{\text{true,cal}}^2(t)} \quad (1)$$

where $V_{\text{obs,cal}}^2$ is the observed visibility squared of the calibrator star, and $V_{\text{true,cal}}^2$ is the intrinsic visibility. If a calibrator star is a point source, then $V_{\text{true,cal}}^2 = 1$ and $V_{\text{system}}^2 = V_{\text{obs,cal}}^2$. For typical observing sequences in optical and IR interferometry, observations of calibrator stars are interleaved with observations of the target star throughout the night to characterize $V_{\text{system}}^2(t)$ over time. Therefore, the intrinsic visibility of the target star measured relative to the system visibility is:

$$V_{\text{true,target}}^2(t) = \frac{V_{\text{obs,target}}^2(t)}{V_{\text{system}}^2(t)} \quad (2)$$

where $V_{\text{obs,target}}^2$ is the observed visibility of the target star. Thus, it is crucial to estimate $V_{\text{system}}^2(t)$ at any given time. Many calibrator stars however have the potential to be slightly resolved by the longest, most scientifically interesting baselines of the interferometer, so $V_{\text{true,cal}}^2 \neq 1$ for these baselines. We must compute $V_{\text{true,cal}}^2$ for the calibrator star given its true angular diameter, θ_{cal} . However, θ_{cal} often is not directly measured by an interferometer given that most calibrator stars are chosen because they are too small to be fully resolved by the longest baselines. Fortunately we can estimate θ_{cal} from the star’s reddening corrected bolometric flux and effective temperature:

$$\theta = (F_{\text{bol}}/\sigma T_{\text{eff}}^4)^{1/2} \quad (3)$$

where σ is the Stefan-Boltzmann constant, and F_{bol} has units of $\text{erg cm}^{-2} \text{s}^{-1}$.

3. METHODS AND DATA

3.1. SED Fitting

In order to obtain accurate stellar angular sizes, each star was fit with a model spectral energy distribution using the fitting routine `sedFit`, written by A. Boden (van Belle & von Braun 2009; van Belle et al. 2016). `sedFit` uses an effective temperature T_{eff} on input, which is mapped to a corresponding Pickles (Pickles 1998) spectral template. `sedFit` then fits the spectral template using the photometry of a given star, to compute the bolometric flux, F_{bol} , and reddening, A_V .

3.2. Target Selection and Catalog Construction

We compiled a list of positions, spectral types and visual magnitudes for ~ 3000 bright ($V_{\text{mag}} < 6$) stars in the northern

hemisphere with declinations $-15^\circ < \delta < 82^\circ$ using the SIMBAD database¹ (Wenger et al. 2000). We chose a brightness limit ($V_{\text{mag}} < 6$) given that most visible light interferometers can obtain scientifically useful data on bright stars. We also removed any stars which appear in the JMMC bad calibrator list.

3.2.1. Removal of Binaries

We purged our list of all known binary and multiple stellar systems. The visibility varies as a function of baseline with the orbital separation and flux ratio for binary systems. Hence, these systems are not suitable as calibrators. We cross-referenced our list of calibrator stars with multiple binary star catalogs to be thorough. We conservatively remove all stars in our list that have an orbit listed in the 9th Catalogue of Spectroscopic Binary orbits (Pourbaix et al. 2004). We also removed all stars that were listed as binaries in the Washington Double Star Catalog (WDS, (Mason et al. 2001)) with separations $\lesssim 2''$ and with flux ratios of $\gtrsim 3$ mag. We also performed a search for any interferometric binaries present in the literature that could be discarded from our list of calibrators. Finally, we removed any objects that were flagged as binaries with $\lesssim 2''$ separation and with flux ratios of $\gtrsim 3$ mag from Hipparcos (van Leeuwen 2007) or the stellar multiplicity catalog of bright stars (Eggleton & Tokovinin 2008). It is possible that a few unknown binary or multiple star systems that are only detectable via interferometry (not via radial velocity) may remain in our calibrator sample. These objects will be removed from our sample as they are observed by visible-light interferometers, such as VISION (Garcia et al. 2016).

3.2.2. Spectral Types

Given that the star’s assumed effective temperature is important to estimating an accurate angular diameter, we obtained spectral types for each star from the Skiff Catalogue of Stellar Spectral Classifications² (Skiff 2009). This catalogue allowed us to determine an accurate spectral type for each star by presenting us with a history of spectral classifications for each object throughout the literature. Occasionally, some ($\sim 10\%$) of the stars in our list did not have spectral types in the Skiff catalog. For these cases, we used the SIMBAD spectral type. For our SED fitting with `sedFit`, we used a Pickles (Pickles 1998) spectral template for each star that was closest to the spectral type and luminosity class obtained from the Skiff catalog or SIMBAD. Pickles spectral template files did not exist for every stellar spectral type. We created these missing templates by averaging two existing, closely related source templates. For example, to create a missing template of spectral type K3V, we averaged the K2V and K4V Pickles spectral templates. We also averaged the assumed effective temperatures of the source templates to estimate the effective temperature of the missing template, with the temperature errors propagating in quadrature.

3.2.3. Uncertainty in Spectral Types and Luminosity Classes for Catalog Stars

Many of our bright stars are Morgan Keenan spectral standards. For these stars, we assumed no uncertainty in the spectral type. Many stars in our list had spectral types and luminosity classes from the Skiff catalog that are inconsistent across

¹ <http://simbad.u-strasbg.fr/simbad/>

² <http://cdsarc.u-strasbg.fr/viz-bin/Cat?B/mk>

Table 2
A Summary of our Calibrator Catalog

Total Stars	Median θ_{LD} (mas)	Median θ_{LD} (% Error)	Median F_{bol} (% Error)	Median V_{mag}	Median χ_{red}^2	Median # of Phot. Points	Median Dist. (pc)	Median A_V
1523	0.527	6.847	1.991	5.49	1.42	15	92.68	0.130

Table 3
Angular Diameters for 1510 Calibrator Stars Estimated from the *sedFit* Fitting Routine along with the χ_{red}^2 as a Quality Flag

HD#	V (mag)	$f_{bol} \pm \sigma$ ($\times 10^{-8}$ erg cm^{-2} s^{-1})	$A_V \pm \sigma$ (mag)	# of Phot. Pts	$\theta_{SED} \pm \sigma$ (mas)	χ_{red}^2	SpT
HD87	5.51	18.900 \pm 1.041	0.023 \pm 0.046	17	0.893 \pm 0.061	1.42	G5III
HD144	5.59	25.890 \pm 0.436	0.205 \pm 0.020	13	0.227 \pm 0.041	6.90	B9III
HD360	5.99	15.830 \pm 2.135	0.236 \pm 0.078	10	0.896 \pm 0.094	1.08	G9III
HD432	2.27	322.300 \pm 6.311	0.085 \pm 0.018	33	1.990 \pm 0.115	1.21	F1IV
HD448	5.53	22.950 \pm 1.920	0.177 \pm 0.058	13	1.110 \pm 0.076	0.83	K0III
HD560	5.51	20.050 \pm 0.261	0.000 \pm 0.020	12	0.214 \pm 0.032	2.36	B9V
HD571	5.03	34.800 \pm 0.975	0.417 \pm 0.018	37	0.656 \pm 0.048	1.23	F2II
HD587	5.84	15.420 \pm 0.991	0.000 \pm 0.053	18	0.913 \pm 0.057	1.17	K0III
HD11946	5.26	21.810 \pm 1.681	0.000 \pm 0.065	9	0.281 \pm 0.021	1.82	A0V
HD11949	5.69	18.710 \pm 1.108	0.073 \pm 0.045	23	1.010 \pm 0.062	0.92	K0III
HD11973	4.79	32.400 \pm 0.962	0.118 \pm 0.025	26	0.592 \pm 0.053	0.99	A9.75IV
HD12139	5.87	19.060 \pm 2.237	0.421 \pm 0.069	9	0.952 \pm 0.065	0.51	K0IV
HD12216	3.98	77.200 \pm 2.180	0.066 \pm 0.026	25	0.567 \pm 0.045	1.08	A1V
HD12230	5.38	22.010 \pm 0.264	0.178 \pm 0.021	11	0.494 \pm 0.013	0.51	F0V
HD12235	5.88	10.740 \pm 0.074	0.000 \pm 0.013	21	0.532 \pm 0.023	5.87	G1IV
HD12303	5.04	59.120 \pm 0.681	0.225 \pm 0.014	28	0.252 \pm 0.061	2.73	B7III
HD12339	5.22	30.030 \pm 1.930	0.173 \pm 0.045	19	1.160 \pm 0.107	0.88	G6.5III
HD12446	5.23	83.700 \pm 9.946	1.284 \pm 0.083	7	0.642 \pm 0.067	0.95	A2IV
HD12447	5.23	82.800 \pm 3.100	0.000 \pm 0.040	8	0.628 \pm 0.030	2.20	A2V
HD51000	5.89	14.640 \pm 1.987	0.214 \pm 0.092	9	0.722 \pm 0.081	0.94	G3III
HD51104	5.92	18.630 \pm 0.226	0.000 \pm 0.025	10	0.171 \pm 0.029	1.03	B8V
HD51250	5.00	54.150 \pm 11.040	0.285 \pm 0.125	8	2.030 \pm 0.230	2.51	K2III
HD51814	5.97	16.670 \pm 2.874	0.353 \pm 0.092	6	0.890 \pm 0.093	0.96	G8III
HD52312	5.96	15.170 \pm 0.170	0.000 \pm 0.027	10	0.173 \pm 0.031	2.42	B9III
HD52497	5.18	34.860 \pm 4.167	0.317 \pm 0.064	16	1.210 \pm 0.104	1.19	G5III
HD52556	5.74	26.470 \pm 7.244	0.571 \pm 0.117	8	1.200 \pm 0.176	1.32	K0III
HD225003	5.63	13.890 \pm 0.079	0.072 \pm 0.017	14	0.393 \pm 0.010	1.35	F0V
HD225180	5.88	35.530 \pm 0.621	1.161 \pm 0.018	12	0.380 \pm 0.070	3.75	A1.5III
HD225216	5.67	23.320 \pm 2.593	0.398 \pm 0.060	8	1.160 \pm 0.077	0.98	K1IV
HD225289	5.80	27.510 \pm 0.402	0.182 \pm 0.023	11	0.172 \pm 0.041	1.66	B7III

This table is available in its entirety in machine-readable form.

the literature. For each of these stars, we used *sedFit* with a grid of spectral types and luminosity classes. The size of the grid corresponded to the range of spectral classifications presented across the literature. The resulting fluxes, as well as the angular diameters, presented in Table 3 are the values from the SED fit that yielded a reduced χ^2 value closest to 1.0.

As an additional check, we tested *sedFit* using Pickles spectral templates with luminosity class I or II, II or III, III or IV, and IV or V. We note that the spectral template used made a significant difference in the estimates of the angular diameters of the giant, bright giant, and supergiant stars (luminosity classes III, II, I, Table 1). The angular diameter estimates for the subgiants and main sequence stars (luminosity classes IV, V) did not change significantly (Table 1) upon using spectral templates with different luminosity class. The spectral types listed in Table 3 represent the model templates that resulted in the highest quality fit.

3.3. Literature Photometry Quality Control

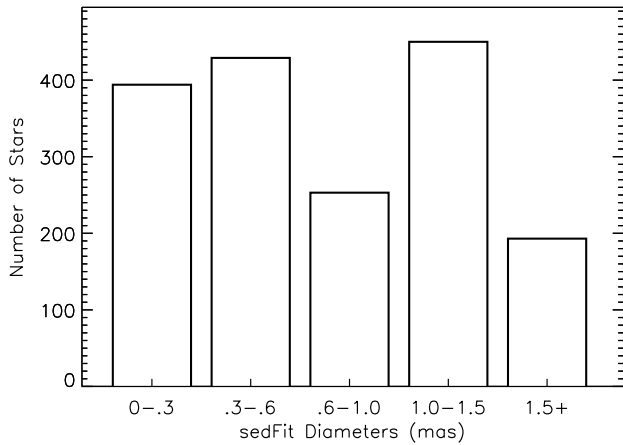
Both broadband and narrowband photometry was obtained for each star by querying both the SIMBAD (Wenger et al. 2000) and General Catalog of Photometric Data (GCPD, (Mermilliod et al. 1997)) online databases. The photometry for a

given star can span 0.2 – 10 μm , and contain multiple photometric systems, such as Johnson (Johnson & Morgan 1953), Strömberg (Strömberg 1956), Villinius (North 1980), DDO (McClure 1976), Geneva (Golay 1972), 13 color (Johnson & Mitchell 1975), and 2MASS (Skrutskie et al. 2006) and IRAS (Beichman et al. 1988) for near to far infrared bands.

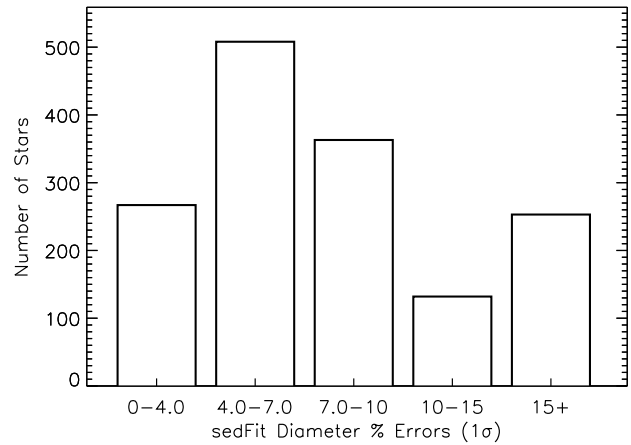
For a small percentage of stars, photometric bandpasses had a significant amount of redundancy, due to multiple photometric catalogs including the same bandpass. These duplicated photometry measurements caused *sedFit* to improperly weight bandpasses during the fitting procedure. We removed these duplicate photometric measurements for all stars in our list.

Furthermore, some stars had poor quality photometric measurements that were far outliers to the SED of the star. These outliers often biased the fitting procedure, yielding inaccurate angular diameters and poor quality (i.e. high reduced χ^2 values) fits to the SED. We removed these poor quality photometry using two criteria. First we removed outliers with photometric magnitudes that were < 0.0 or > 10.0 . Second, we removed photometric measurements obtained from different catalogs in the same bandpass that varied by more than 1.2 σ .

Although this method of cleaning the photometry yielded

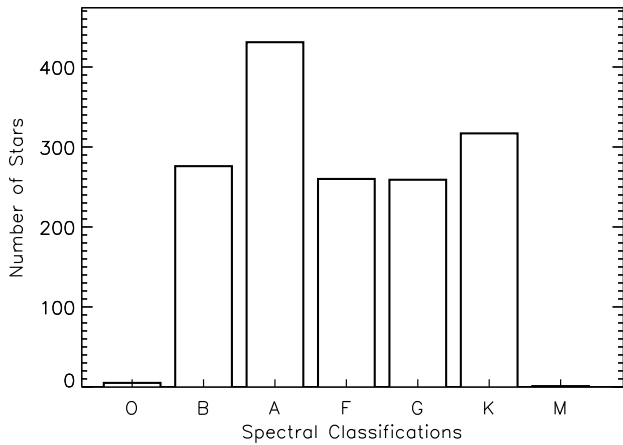


(a) Angular Diameters

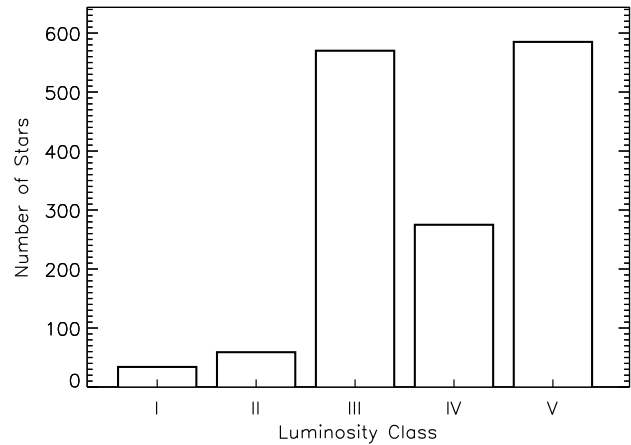


(b) Angular Diameter Errors (1 σ)

Figure 1. Distributions of angular diameters and 1 σ errors obtained using *sedFit*, within our sample of 1523 stars. All of our calibrator stars have fitted angular diameters < 2.5 mas, given that larger (> 2.5 mas) stars are usually resolved by visible-light interferometers. The median error on our fitted angular diameters is 6.789%.



(a) Spectral Types



(b) Luminosity Classes

Figure 2. Distributions of spectral types and luminosity classes for our calibrator stars (see §3.2.2)

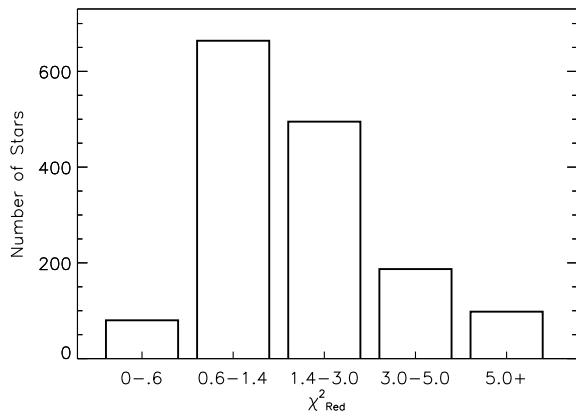


Figure 3. Reduced chi square χ^2_{red} for the SED fits to literature photometry for each calibrator star in our sample.

much better fits to most of the stellar SEDs, there were still many fits with large reduced χ^2 values due to problematic photometry. Therefore, we developed an objective criterion based on reduced χ^2 (χ^2_{ν}) as follows. Using the set of 75 interferometric comparison stars from prior literature (see Section 5), we found that the residuals between our estimated angular diameters and the interferometric values roughly follows the relation $\Delta\theta/\theta_{\text{lit}} \sim 0.04 + 0.009 \times \chi^2_{\nu}$, where θ_{lit} is the interferometrically measured angular diameter from the literature. Therefore, we opted to define an empirical threshold such that we retained only stars with $\chi^2_{\nu} \leq 7.0$. This corresponds to an expected fractional error on θ of at most $\sim 10\%$, and represents only a mild extrapolation from the range of χ^2_{ν} spanned by the 75 comparison stars (the worst outlier among the comparison set has $\chi^2_{\nu} = 5.0$).

4. RESULTS

We present a list of 1523 interferometric calibrator stars culled from all stars $V < 6$ in the northern hemisphere (see §3.2). Angular diameters were estimated from the SED fitting routine *sedFit* (see §3.1). The median angular diameter

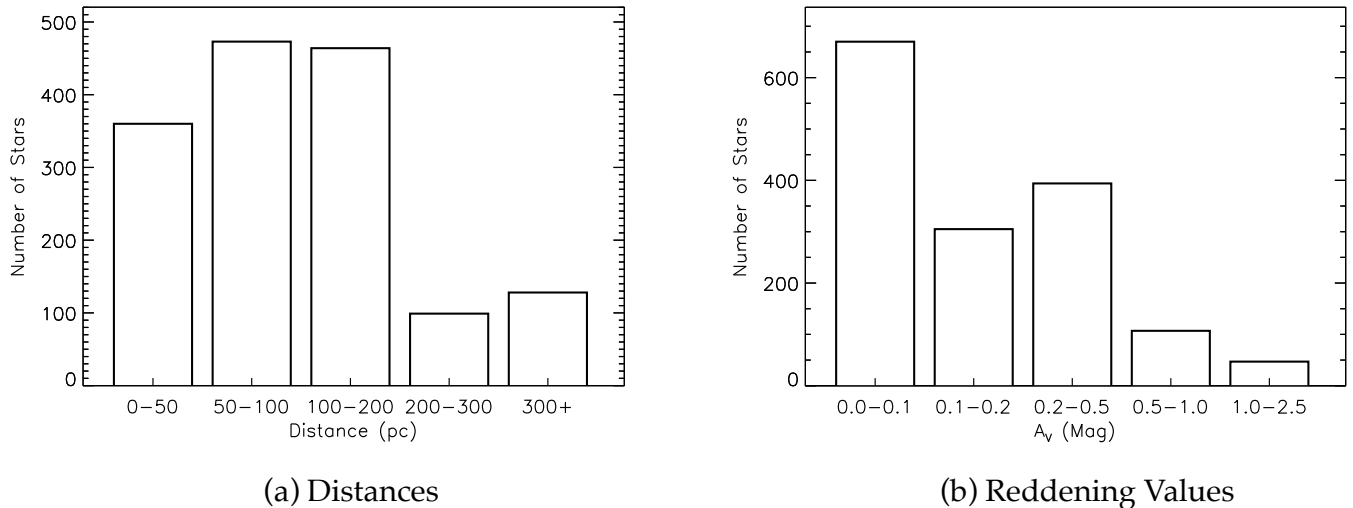


Figure 4. Distributions of Hipparcos distances and reddening values from our sample of calibrator stars. The majority of our bright $V < 6$ mag stars are nearby (< 300 pc). Therefore, most calibrator stars are expected to have low reddening $A_V < 1$.

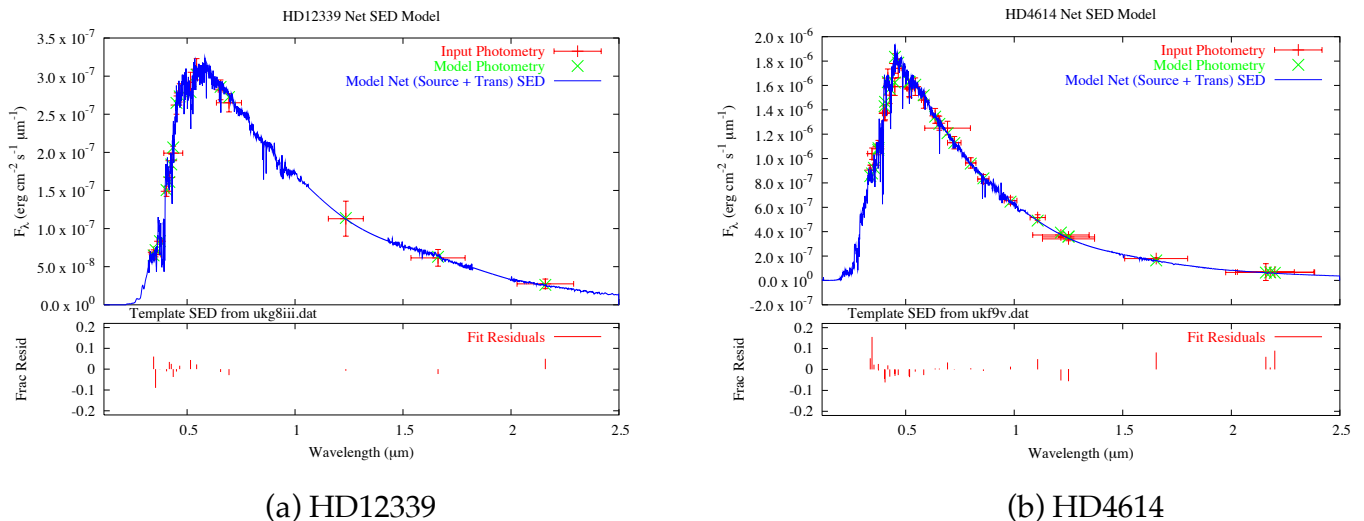


Figure 5. Example spectral energy distribution (SED) plots for HD 12339 and HD 4614. Literature photometry (red crosses) are fit by model photometry (green X's) derived from `sedFit` using a scaled, reddened spectral template (blue line) from Pickles (1998) (see §3.1) corresponding to the star's known spectral type (see §3.2.2). `sedFit` minimizes the residuals between the literature photometry and the model photometry. The complete figure set (1510 images) is available in the online journal.

θ_{SED} of stars in our calibrator list is 0.527 mas, while the median reduced $\chi^2_{\text{median,red}}$ value for all our fits is 1.42. We present the source bolometric flux, F_{bol} , used for all fits as well as reddening, A_V . A brief summary of our catalog can be found in Table 2. The full table is presented in Table 3. The distributions of angular diameters and their errors, spectral types and luminosity classes, best-fit metrics, distances, and reddening values within our sample are displayed in Figure 1 through Figure 4 respectively. Two example SED fits for G8III giant HD12339 and F9V main sequence star HD4614 are shown in Figure 5. See Appendix for fits to the SEDs for all stars in our catalog.

4.1. Assessing Quality of the Fits

From our initial large number (2191) of bright stars vetted for binaries for which we derived angular diameters, many had poor fits due to poor-quality photometry even after we removed much of the photometric outliers from each well-characterized SED (see §3.3). To further improve the reliability

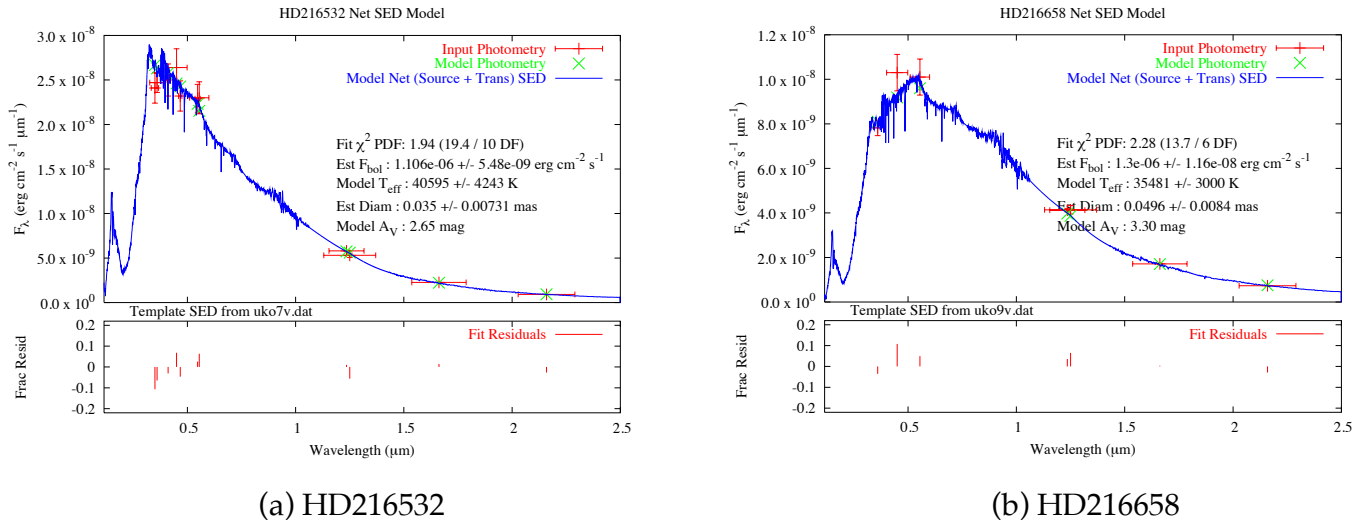
of our calibrator star angular diameters, we first remove any stars from our calibrator catalog (Table 3) that had either of the following criteria:

- Stars with $\theta_{\text{SED}} > 2.5$ mas are excluded because they are resolved by most visible-light interferometers.
- Stars with < 4 photometry data points are excluded because the SEDs were poorly constrained.

These cuts removed 307 stars from our sample. Next, as described above, we removed any stars with reduced χ^2 value greater than 7.0. All of the remaining stars have low reduced χ^2 values and have been assessed to be well-fit (see Appendix for the SED fits). These checks removed an additional 361 stars, to arrive at our sample of 1523 total stars.

4.2. Check on Accuracy of Derived Reddening A_V

Given that the majority (92%) of our stars are within 300 pc as shown in Figure 4a, we expect the median reddening of our



(a) HD216532

(b) HD216658

Figure 6. Example SED fits to two OB stars in the Cep-OB3 association with directly measured extinction curves by [Massa & Savage \(1984\)](#). Our best-fit reddening of $A_V = 2.65$ mag for O7V star HD216532 and $A_V = 3.30$ mag for O9V star HD216658 using `sedFit` are in good agreement with [Massa & Savage \(1984\)](#) directly-observed reddening of $A_V = 2.66$ and $A_V = 3.03$, respectively.

Table 4
We Validate our SED-Fitting Methods by Deriving the Reddening A_V using `sedFit` for 21 OB Stars in the Cep OB3 Cloud.

HD/ALS#	$f_{\text{bol}} \pm \sigma$ ($\times 10^{-8}$ erg cm $^{-2}$ s $^{-1}$)	$A_V \pm \sigma$ (mag)	# of Phot. Pts	$\theta_{\text{SED}} \pm \sigma$ (mas)	χ^2_{red}	SpT	A_V Massa84
ALS12680	54.33 \pm 0.89	2.60 \pm 0.05	10	0.05 \pm 0.01	0.85	B0V	2.418
ALS12682	23.31 \pm 0.30	2.75 \pm 0.05	11	0.06 \pm 0.02	3.34	B2V	3.069
ALS12732	18.51 \pm 0.27	2.15 \pm 0.05	10	0.05 \pm 0.02	1.76	B2V	2.387
ALS12736	19.98 \pm 2.94	2.90 \pm 0.15	6	0.06 \pm 0.01	2.57	B12III	2.945
ALS12766	18.38 \pm 0.45	2.10 \pm 0.08	11	0.05 \pm 0.02	4.10	B2V	2.294
ALS12865	24.34 \pm 0.31	1.60 \pm 0.05	6	0.07 \pm 0.01	3.98	B12III	1.798
ALS12867	76.35 \pm 1.05	2.80 \pm 0.07	6	0.12 \pm 0.02	0.73	B12III	3.131
HD216532	110.60 \pm 1.35	2.65 \pm 0.05	11	0.04 \pm 0.01	1.94	O7V	2.666
HD216658	130.00 \pm 2.45	3.30 \pm 0.07	7	0.05 \pm 0.01	2.28	O9V	3.038
HD216711	35.68 \pm 0.37	2.60 \pm 0.05	9	0.08 \pm 0.02	3.42	B2V	2.728
HD216898	104.00 \pm 20.60	2.60 \pm 0.05	12	0.03 \pm 0.01	2.92	O7V	2.635
HD217061	52.82 \pm 0.44	2.70 \pm 0.05	11	0.09 \pm 0.03	5.31	B2V	2.976
HD217086	202.80 \pm 42.85	2.95 \pm 0.10	8	0.05 \pm 0.01	1.13	O7V	2.976
HD217297	64.87 \pm 1.12	1.55 \pm 0.07	11	0.10 \pm 0.03	3.06	B2V	1.767
HD217312	164.40 \pm 1.65	2.10 \pm 0.05	7	0.06 \pm 0.01	3.71	O9V	2.046
HD217463	28.31 \pm 0.48	2.30 \pm 0.05	11	0.07 \pm 0.02	1.40	B2V	2.449
HD217657	112.50 \pm 2.95	2.35 \pm 0.10	9	0.05 \pm 0.01	1.69	O9V	2.387
HD217979	23.25 \pm 0.27	1.65 \pm 0.05	11	0.06 \pm 0.02	4.01	B2V	1.891
HD218066	75.37 \pm 2.31	1.95 \pm 0.10	7	0.11 \pm 0.03	1.12	B2V	2.015
HD218323	96.76 \pm 2.59	2.35 \pm 0.08	11	0.14 \pm 0.02	1.70	B12III	2.790
HD218342	87.85 \pm 1.72	1.95 \pm 0.05	14	0.13 \pm 0.02	2.06	B12III	2.232

Note: Our derived A_V for each star (column 3) agree well with the directly observed A_V (last column) for these stars using the IUE satellite (See Table 2, 4th column, [Massa & Savage 1984](#)).

sample to be $A_V < 0.3$. Figure 4b shows the reddening of our sample, with a median reddening of $A_{V,\text{med}} = 0.13$, in good agreement with expectations.

As a check on the accuracy of derived reddening A_V from `sedFit`, we use the sample of 21 OB stars in the Cep OB3 association with directly observed UV extinction curves from the International Ultraviolet Explorer (IUE, [Bogess et al. 1978](#)) satellite observations ([Massa & Conti 1981](#); [Massa & Savage 1984](#)). We fit the SEDs of 21 stars from photometry derived from the literature, in the same manner as §3. Example SED fits to stars in the Cep OB3 association for HD216532 and HD216658 are shown in Figure 6.

We perform 160 fits for each star, with the reddening parameter spanning $A_V = 0.0 - 4.0$ in steps of 0.05. For each

star, similar to the methods detailed in §3.1, we identify the best-fit model as the one with reduced χ^2 closest to 1.0 ([Andrae et al. 2010](#)). To estimate the uncertainty on our derived reddening, we compute a 5σ confidence interval, identifying models where $\Delta\chi^2_{99.73\%} = 11.8 < \chi^2 - \chi^2_{\text{best}}$, where χ^2_{best} corresponds to the the best-fit model, and $\Delta\chi^2_{99.73\%} = 11.8$ corresponds to models that fall within the 5σ confidence interval (see section 15.6, [Press et al. 2002](#)).

As shown in Table 4 and Figure 7, we find our fitted A_V for 21 stars in good agreement with the directly observed A_V for each star from [Massa & Savage \(1984\)](#) (c.f. 4th column, Table 2), with a mean offset in the reddening of -0.13 ± 0.17 mag, demonstrating good agreement. This small systematic offset in reddening should not significantly affect

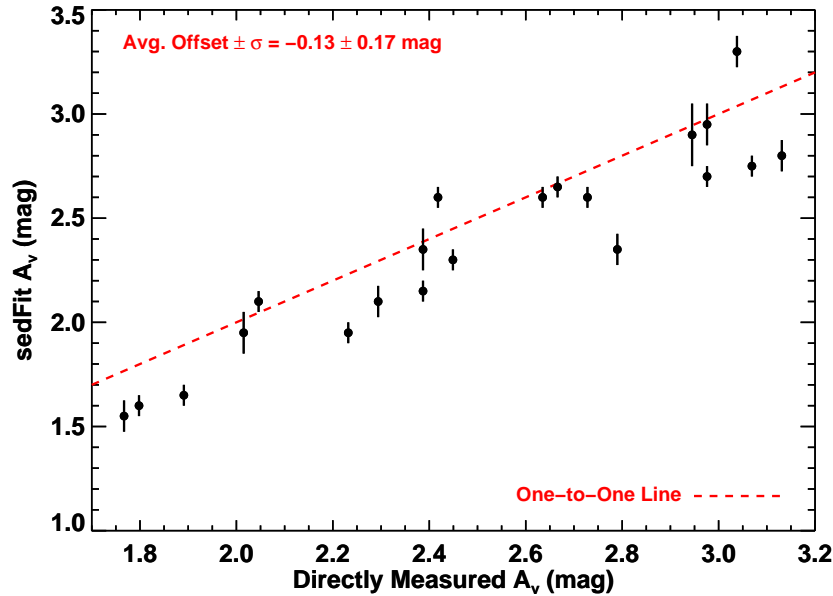


Figure 7. We validate our SED-fitting method by comparing the reddening A_V using `sedFit` for 21 OB stars in the Cep OB3 cloud (Y-axis) to the directly observed A_V for these stars using the IUE satellite (See Table 2, 4th column, [Massa & Savage 1984](#)). We find a statistically insignificant average offset of -0.13 ± 0.17 mag.

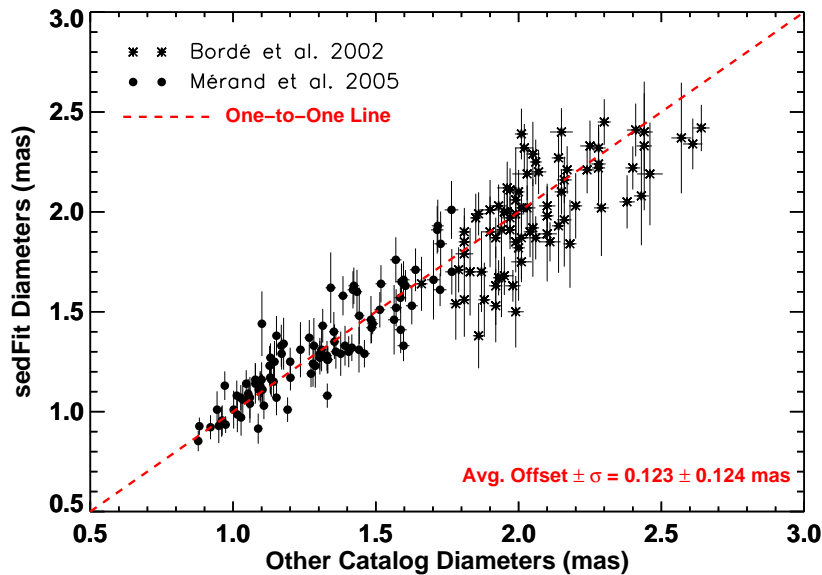


Figure 8. Comparison of estimated angular diameters from this work and those estimated by previous calibrator catalogs from [Bordé et al. \(2002\)](#) and [Mérand et al. \(2005\)](#) (see § 5). There is a statistically insignificant offset of 0.123 ± 0.124 mas between our angular diameters and previous catalogs. Despite the hundreds of stars in each catalog, there are few stars in common, given that [Bordé et al. \(2002\)](#) and [Mérand et al. \(2005\)](#) optimized their catalogs for infrared interferometry – our calibrator catalog is optimized for visible-light interferometry.

the accuracy of the derived angular diameters of our calibrator stars, as we now show.

5. DISCUSSION: COMPARISON TO PREVIOUS CATALOGS

Several authors have previously presented catalogs of interferometric calibrators, including e.g., [Bordé et al. \(2002\)](#), [Mérand et al. \(2005\)](#), [Bonneau et al. \(2006\)](#), [van Belle et al. \(2008\)](#), and [Richichi et al. \(2009\)](#). These catalogs were optimized for infrared interferometry, as appropriate for infrared beam combiners on the Very Large Telescope Interferometer and the CHARA array. Our catalog builds on these previous works, and extends them by optimizing a calibrator sample for the optical, as is needed by next-generation interferometers

such as VISION at NPOI (e.g., [Garcia et al. 2016](#)). Furthermore, of the 1523 stars in our sample, there are only 97 stars in common with the [Mérand et al. \(2005\)](#) catalog, while only 79 overlap with [Bordé et al. \(2002\)](#), showing we have greatly expanded the potential calibrator pool. In Figure 8 we compare our angular diameter estimates to those of [Mérand et al. \(2005\)](#) and [Bordé et al. \(2002\)](#), finding them in good agreement with no statistically significant systematic offset. These works focused on larger potential calibrator stars that were optimal for 200-m class (and smaller) interferometers working in IR bands, while the vast majority of our catalog contains stars smaller than 1.0 milliarcsecond (Figure 1), which are ideal for

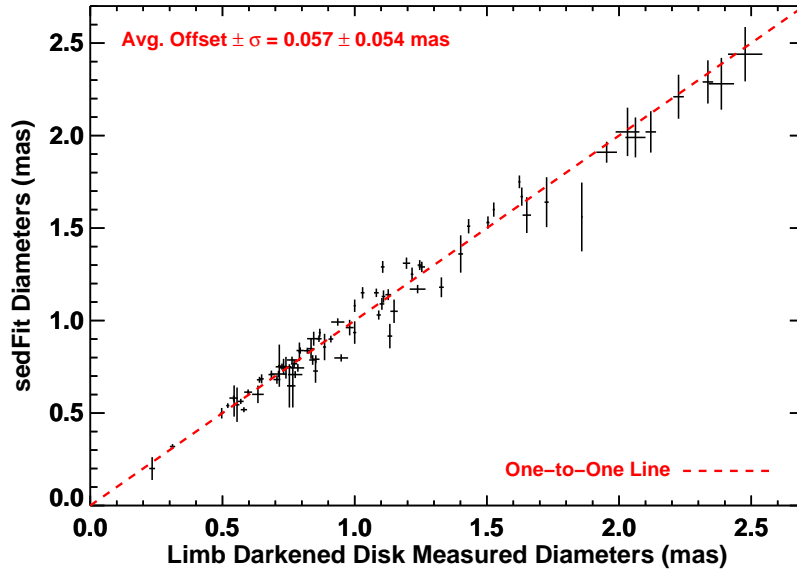


Figure 9. Comparison of estimated angular diameters from *sedFit* and those measured interferometrically from the literature (see Table 5). Each cross is the angular diameter for a calibrator star estimated with *sedFit* and its corresponding directly measured limb darkened disk angular diameter from the literature.

Table 5
sedFit Angular Diameters Compared to Angular
 Diameters Measured by Interferometers.

HD#	$\theta_{LD} \pm \sigma$ (mas)	$\theta_{SED} \pm \sigma$ (mas)	REF
HD3360	0.311 ± 0.010	0.319 ± 0.013	4
HD4614	1.623 ± 0.004	1.750 ± 0.035	1
HD4628	0.868 ± 0.004	0.934 ± 0.022	2
HD5015	0.865 ± 0.010	0.902 ± 0.018	1
HD6210	0.520 ± 0.006	0.540 ± 0.013	3
HD10476	1.000 ± 0.004	1.080 ± 0.034	3
HD10780	0.763 ± 0.019	0.787 ± 0.018	1
HD16160	1.030 ± 0.007	1.150 ± 0.031	2
HD33564	0.640 ± 0.010	0.680 ± 0.016	8
HD34411	0.981 ± 0.015	0.962 ± 0.042	1
HD35468	0.715 ± 0.005	0.756 ± 0.114	6
HD161797	1.953 ± 0.039	1.910 ± 0.057	7
HD162003	0.949 ± 0.026	0.798 ± 0.020	1
HD164259	0.775 ± 0.027	0.708 ± 0.019	1
HD170693	2.120 ± 0.020	2.020 ± 0.112	5
HD173667	1.000 ± 0.006	0.935 ± 0.061	1
HD176437	0.753 ± 0.009	0.647 ± 0.117	4
HD176437	0.766 ± 0.010	0.647 ± 0.117	6
HD219623	0.542 ± 0.016	0.581 ± 0.013	3
HD222368	1.082 ± 0.009	1.150 ± 0.023	1
HD222603	0.581 ± 0.012	0.518 ± 0.014	3

References. ¹Boyajian et al. (2012a), ²Boyajian et al. (2012b), ³Boyajian et al. (2013), ⁴Maestro et al. (2013), ⁵Ligi et al. (2012), ⁶Challouf et al. (2014), ⁷Mozurkewich et al. (2003), ⁸von Braun et al. (2014), ⁹Baines et al. (2009), ¹⁰Baines et al. (2010). A full version of this table is available online.

the longest (> 300-m) baselines on next-generation optical interferometers.

For our purposes here, we can also utilize previous interferometric observations as a check on the accuracy of our limb-darkened angular diameter estimates, θ_{LD} . Specifically, we compare 75 stars from our list to their interferometrically measured diameters from the literature (Mozurkewich et al. 2003; Baines et al. 2009, 2010; Ligi et al. 2012; Boyajian et al. 2012a,b, 2013; Maestro et al. 2013; Challouf et al. 2014; von Braun et al. 2014) in Table 5 and Figure 9. Our angular diame-

ter estimates are in excellent agreement with those measured interferometrically, with a mean offset of 0.057 ± 0.054 mas. There is no systematic offset between our estimated calibrator star angular diameters from *sedFit* and their corresponding measured angular diameters from the literature.

6. SUMMARY

Of the ~ 3000 stars in the northern hemisphere brighter than $V < 6$ and with declinations $-15^\circ < \delta < 82^\circ$, we have compiled a list of 1523 stars well suited as interferometric calibrators, with *uniformly* estimated angular diameters and bolometric fluxes from SED fitting. Each star was fit with a model SED, including a reddening correction, to literature photometry spanning $0.2 - 10 \mu\text{m}$, using a spectral template on input, corresponding to a specific spectral type. We purged this list of known binary and multiple stellar systems, stars with poor-quality or sparse photometry, and stars where the spectral template fit resulted in a poor reduced χ^2 .

For a subset of the stars in our sample, our derived angular diameters show excellent agreement with directly measured angular diameters from the literature, and with diameter estimates appearing in previous calibrator catalogs. In addition, our derived reddening for OB stars in the Cep OB3 association show excellent agreement with directly measured reddening for those stars from the literature.

With the next generation of interferometers that operate at visible wavelengths now operating and more coming online, this catalog should serve as a broadly useful resource for years to come.

ACKNOWLEDGEMENTS

We thank the anonymous referee for helpful critiques that improved the clarity and quality of this paper. S.J.S. would like to thank the NSF REU program at Vanderbilt University for the opportunities and support that made this work possible. E.V.G. and K.G.S. gratefully acknowledge partial support from NSF PAARE grant AST-1358862. This research has made use of the SIMBAD database, operated at CDS, Strasbourg, France. This research has made use of the Washington Double Star

Catalog maintained at the U.S. Naval Observatory.

REFERENCES

- Andrae, R., Schulze-Hartung, T., & Melchior, P. 2010, ArXiv e-prints, arXiv:1012.3754
- Armstrong, J. T., Mozurkewich, D., Rickard, L. J., et al. 1998, ApJ, 496, 550
- Baines, E. K., McAlister, H. A., ten Brummelaar, T. A., et al. 2009, ApJ, 701, 154
- Baines, E. K., Döllinger, M. P., Cusano, F., et al. 2010, ApJ, 710, 1365
- Beichman, C. A., Neugebauer, G., Habing, H. J., Clegg, P. E., & Chester, T. J., eds. 1988, *Infrared astronomical satellite (IRAS) catalogs and atlases. Volume 1: Explanatory supplement*, Vol. 1
- Bogges, A., Carr, F. A., Evans, D. C., et al. 1978, Nature, 275, 372
- Bonneau, D., Clause, J.-M., Delfosse, X., et al. 2006, A&A, 456, 789
- Bordé, P., Coudé du Foresto, V., Chagnon, G., & Perrin, G. 2002, A&A, 393, 183
- Boyajian, T. S., McAlister, H. A., van Belle, G., et al. 2012a, ApJ, 746, 101
- Boyajian, T. S., von Braun, K., van Belle, G., et al. 2012b, ApJ, 757, 112
- . 2013, ApJ, 771, 40
- Challouf, M., Nardetto, N., Mourard, D., Aroui, H., & Delaa, O. 2014, in SF2A-2014: Proceedings of the Annual meeting of the French Society of Astronomy and Astrophysics, ed. J. Ballet, F. Martins, F. Bournaud, R. Monier, & C. Reylé, 471–474
- Eggleton, P. P., & Tokovinin, A. A. 2008, MNRAS, 389, 869
- Garcia, E. V., Muterspaugh, M. W., van Belle, G., et al. 2016, PASP, 128, 055004
- Ghasempour, A., Muterspaugh, M. W., Hutter, D. J., et al. 2012, in Society of Photo-Optical Instrumentation Engineers (SPIE) Conference Series, Vol. 8445, Society of Photo-Optical Instrumentation Engineers (SPIE) Conference Series, 0
- Golay, M. 1972, Vistas in Astronomy, 14, 13
- Ireland, M. J., Mérand, A., ten Brummelaar, T. A., et al. 2008, in Society of Photo-Optical Instrumentation Engineers (SPIE) Conference Series, Vol. 7013, Society of Photo-Optical Instrumentation Engineers (SPIE) Conference Series, 24
- Johnson, H. L., & Mitchell, R. I. 1975, Rev. Mexicana Astron. Astrofis., 1, 299
- Johnson, H. L., & Morgan, W. W. 1953, ApJ, 117, 313
- Ligi, R., Mourard, D., Lagrange, A. M., et al. 2012, A&A, 545, A5
- Maestro, V., Che, X., Huber, D., et al. 2013, MNRAS, 434, 1321
- Mason, B. D., Wycoff, G. L., Hartkopf, W. I., Douglass, G. G., & Worley, C. E. 2001, AJ, 122, 3466
- Massa, D., & Conti, P. S. 1981, ApJ, 248, 201
- Massa, D., & Savage, B. D. 1984, ApJ, 279, 310
- McClure, R. D. 1976, AJ, 81, 182
- Mérand, A., Bordé, P., & Coudé du Foresto, V. 2005, A&A, 433, 1155
- Mermilliod, J.-C., Mermilliod, M., & Hauck, B. 1997, A&AS, 124, 349
- Monnier, J. D., Berger, J.-P., Millan-Gabet, R., & ten Brummelaar, T. A. 2004, in Society of Photo-Optical Instrumentation Engineers (SPIE) Conference Series, Vol. 5491, New Frontiers in Stellar Interferometry, ed. W. A. Traub, 1370
- Mourard, D., Clause, J. M., Marcotto, A., et al. 2009, A&A, 508, 1073
- Mozurkewich, D., Armstrong, J. T., Hindsley, R. B., et al. 2003, AJ, 126, 2502
- North, P. 1980, A&AS, 41, 395
- Pickles, A. J. 1998, PASP, 110, 863
- Pourbaix, D., Tokovinin, A. A., Batten, A. H., et al. 2004, A&A, 424, 727
- Press, W. H., Teukolsky, S. A., Vetterling, W. T., & Flannery, B. P. 2002, Numerical recipes in C++ : the art of scientific computing
- Richichi, A., Percheron, I., & Davis, J. 2009, MNRAS, 399, 399
- Skiff, B. A. 2009, VizieR Online Data Catalog, 1, 2023
- Skrutskie, M. F., Cutri, R. M., Stiening, R., et al. 2006, AJ, 131, 1163
- Strömgren, B. 1956, Vistas in Astronomy, 2, 1336
- ten Brummelaar, T. A., McAlister, H. A., Ridgway, S. T., et al. 2005, ApJ, 628, 453
- ten Brummelaar, T. A., Sturmman, J., Ridgway, S. T., et al. 2013, Journal of Astronomical Instrumentation, 2, 40004
- van Belle, G. T., Creech-Eakman, M., & Ruiz-Velasco, A. 2016, ArXiv e-prints, arXiv:1604.00984
- van Belle, G. T., & van Belle, G. 2005, PASP, 117, 1263
- van Belle, G. T., & von Braun, K. 2009, ApJ, 694, 1085
- van Belle, G. T., van Belle, G., Creech-Eakman, M. J., et al. 2008, ApJS, 176, 276
- van Leeuwen, F. 2007, A&A, 474, 653
- von Braun, K., Boyajian, T. S., van Belle, G. T., et al. 2014, MNRAS, 438, 2413
- Wenger, M., Ochsenbein, F., Egret, D., et al. 2000, A&AS, 143, 9